Physical Properties of Barium Titanate-Filled Rubber-Modified Epoxies

MUN-FU TSE,* *AT&T Technologies, Inc., Engineering Research Center, Princeton, New Jersey 08540*

Synopsis

Rubber-modified epoxies (RME) filled with different levels of barium titanate ($BaTiO_3$) have been characterized by using DSC, TGA, and TMA. The presence of the filler does not affect the glass transition temperature or the activation energy of pyrolysis; however, it does change other thermal properties. The dielectric constant increases markedly, but the dissipation factor remains fairly constant with increasing $BaTiO_3$ loading. The polymers, in MEK, exhibit slightly different degrees of swelling and their sol fractions vary. Mechanical properties, such as stress-strain relation, friction, abrasion, scratch hardness, and scrape adhesion of the polymers, will be described.

INTRODUCTION

Epoxy resin-based systems comprise an important class of polymers widely used for protective and electronic-grade coatings. However, the pure polymers have poor fracture properties, such as inferior impact strength and crack resistance. McGarry and coworkers[1-3] discussed the concept of elastomeric reinforcement in thermosetting polymers as a means of enhancing their impact strength and fracture surface energy. Since then a tremendous amount of work[4-8] has been done on the systems of epoxy resin modified with liquid carboxy-terminated butadiene-acrylonitrile copolymer (CTBN).

In this work, a rubber-modified epoxy (RME) has further been modified by the addition of a ceramic filler, barium titanate ($BaTiO_3$), to obtain a polymeric system with a high dielectric constant. The polymer with different levels of filler was then characterized via DSC, TGA, and TMA. Various physical property measurements, such as dielectric constant, dissipation factor, solvent swelling, stress-strain relation, friction, abrasion, scratch hardness, and scrape adhesion, were carried out to gain a better understanding of this particular system of polymeric materials.

EXPERIMENTAL

Materials

The barium titanate, Ticon 5016, manufactured by Tam Ceramics, Inc. (Niagara Falls, New York), is prepared by the solid-state reaction of barium carbonate and titanium oxide. The crystal structure of barium titanate is

* Present address: Exxon Chemical Company, P. O. Box 241, Baton Rouge, Louisiana 70821.

Journal of Applied Polymer Science, Vol. 30, 3625–3647 (1985)

CCC 0021-8995/85/093625-23$04.00

a perovskite structure,[9,10] as shown in Figure 1. The barium and oxygen ions combine to form a face-centered cubic lattice, with the titanium ions occupying the octahedral interstices. When $BaTiO_3$ cools down through the Curie temperature, the symmetrical TiO_6 octahedron changes from cubic to tetragonal symmetry, with the titanium ion in an off-center position corresponding to an electric dipole moment. At this point the dielectric constant and loss tangent go through a maximum and a minimum, respectively.

Some important physical properties[11] of Ticon 5016 are listed in Table I, where the Fisher number is defined as the average equivalent spherical diameter in microns (or μm) of the ceramic, and D_n is the particle size (μm) that is greater than n% of all particles by mass. The material appears in the form of a fine powder, which colors white. The dielectric constant has a maximum and the dissipation factor has a minimum at 130°C, which is the Curie temperature.

Polymer Preparation

The base epoxy resin,[8] in powdered form, contained 7 wt % of a carboxy-terminated butadiene-acrylonitrile copolymer (Hycar Reactive Liquid Polymer, B. F. Goodrich Chemical Company). This Hycar liquid polymer has an acrylonitrile content of 26% and a functionality of 1.8. The base resin was then compounded with different amounts of barium titanate and cured by an accelerated dicyandiamide curing agent. The composition of the different barium titanate-filled materials is shown in Table II.

Sample preparation involved the deposition of the uncured polymer on a 25-mil aluminum panel (Q-Panel Company, Cleveland, Ohio), either via fluidized-bed coating (for RME0, RME10, and RME40 materials) or compression molding (for RME60 material only). Fluidized-bed coating of

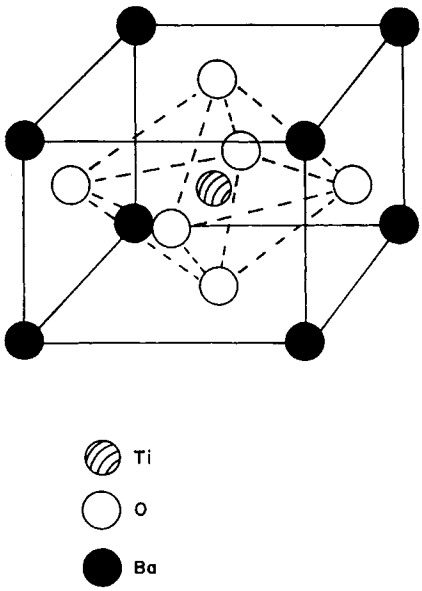

Fig. 1. Ideal perovskite structure.

TABLE I
Physical Properties of Ticon Barium Titanate 5016

Fisher number	1.43
D_{90}	3.6
D_{50}	1.4
D_{10}	0.7
Surface area (m^2/g)	2.30
Dielectric constant, 1 kHz	~1500 (25°C)
	~8000–10,000 (130°C)
Dissipation factor, 1 kHz	~0.010–0.015 (25°C)
	~0.005 (130°C)
Fired density (g/cm^3)	5.5–5.7

RME60 usually yielded a rough surface; compression molding of the same polymer gave a relatively smooth surface. The coated panel was then cured according to the cure schedule, as mentioned in Table II. A free film of the cured material can be obtained by spraying the aluminum panel with a mold release agent (FreKote 33, FreKote, Inc.) before the polymer deposition and peeling the subsequently cured film from the metal substrate. The film thickness was in the range of 74–406 μm (2.9–16.0 mils).

A commercial rubber-modified epoxy, Kelpoxy G293-100 (Spencer Kellogg Division, Textron Inc., Buffalo, New York), was also studied for comparison with the RME polymers. This Kelpoxy polymer, in the form of a very viscous liquid, contains 40 wt % carboxy-terminated butadiene-acrylonitrile copolymer and it has an epoxy equivalent weight (EEW) of 340.[12] Accelerated dicyandiamide, which is in solid form, is difficult to mix homogeneously with the Kelpoxy polymer. Therefore, a 30% (wt/vol) solution of this curing agent in DMF (Fisher Scientific Company) was prepared and blended into the above polymer. Another curing agent, dimethylenetriamine (DETA; J. T. Baker Chemical Company, Phillipsburg, New Jersey) was used. The formulation and cure conditions of the different polymers derived from Kelpoxy G293-100 are shown in Table III.

Epoxy Equivalent Weight Determination

The epoxy equivalent weight of an epoxy resin is the grams of resin containing 1 g Eq of epoxy groups. The EEW of RMEO was measured according to Jay's method.[13] A specimen with weight of about 0.5 g was dissolved in 20 ml of a 1:1 mixture of chloroform and chlorobenzene. To

TABLE II
Composition of Barium Titanate-Filled Rubber-Modified Epoxy

	RME0	RME10	RME40	RME60
Composition				
Powdered epoxy resin	100	100	100	100
Accelerated dicyandiamide	3.3	3.3	3.3	3.3
$BaTiO_3$	0	11.5	69.0	155.0
Wt % $BaTiO_3$	0	10	40	60
Vol % $BaTiO_3$	0	2	7	11
Cure condition	200°C for 15 min			

TABLE III
Formulation of Kelpoxy Polymers

	Kelpoxy 1	Kelpoxy 2	Kelpoxy 3
Formulation			
Kelpoxy G293-100	100	100	100
Accelerated dicyandiamide	9.4[a]	9.4[a]	—
DETA	—	—	6.1
Cure condition	200°C, 15 min	100°C, 2 h; 120°C, 5 h	82°C, 16 h

[a] Dissolved in DMF to make a 30 wt. % solution.

the resin solution was added 20 ml of tetraethylammonium bromide reagent (100 g of Et_4NBr dissolved in 400 ml of glacial acetic acid), and a standard 0.1 *N* perchloric acid was used to titrate the mixture by using a Potentigraph E536 and a Dosimat E535 and E549 (Metrohm Herisau, Switzerland). A blank determination on the reagents was made in an identical manner. The EEW was then calculated as

$$\text{EEW} = \frac{1000\ \text{S}}{\text{N}(V - B)}$$

where S = grams of specimen, N = normality of HBr in acetic acid, V = ml of HBr solution used for titration of the specimen in solution, and B = ml of HBr solution used for titration of the blank.

Thermal Analysis

Differential Scanning Calorimetry (DSC)

DSC measurements were made with a DuPont DSC 910 equipped with a 1090 Thermal Analyzer and a 1091 Disk Memory using nitrogen atmosphere. A sample with a weight of 10–15 mg in an aluminum pan with a cover aligned with respect to the pan was used for each run. The instrument was calibrated for temperature and enthalpy with an indium sample of weight 7–8 mg, run from 120 to 180°C at a heating rate of 5°C/min. The polymer sample runs were also performed at the same heating rate.

First, each uncured polymer in Table II was run from room temperature to 340°C to obtain the heat of reaction of the cross-linking process. Then the sample was cooled to room temperature by itself in the DSC cell without the use of any cooling agent, such as liquid nitrogen. A second thermal scan from room temperature to 340°C was started again to obtain the glass transition temperature of the polymer. The glass transition temperature was taken as the onset of transition in each plot of heat flow versus temperature.

Second, each polymer cured according to the cure schedule shown in Tables II and III was run from room temperature to 250°C. Then the sample was cooled to room temperature, as described above. A second thermal scan from room temperature to 250°C was performed. The sample was then subjected to another identical cooling cycle to room temperature again, and

its temperature was further brought down to −120°C with the use of liquid nitrogen. A final thermal scan from this temperature to 250°C was run.

Thermogravimetric Analysis (TGA)

TGA measurements of the RME polymers from room temperature to 800°C were made with a DuPont TGA 951 equipped with a 1090 Thermal Analyzer and a 1091 Disk Memory. Air atmosphere was used to determine the filler content of each polymer at a heating rate of 10°C/min. On the other hand, nitrogen atmosphere was used to study the activation energy of pyrolysis at heating rates of 5, 10, 15, 20, and 30°C/min. The sample holder was a platinum pan, and the sample weight was monitored to be 15 ± 1 mg.

Thermomechanical Analysis (TMA)

A Perkin-Elmer Model TMS-1 Thermomechanical Analyzer was used to perform thermal scans of the RME polymers from 0 to 200°C. The linear expansion probe, loaded with 4 g (for compensating probe buoyancy), was rested on a sample and pushed up as the sample expanded at a heating rate of 10°C/min in a helium atmosphere. A sloping plot of length against temperature was obtained, with the gradient proportional to the thermal expansion coefficient of the sample. It was necessary to scan each sample once through the whole temperature range to eliminate any incomplete chemical reaction left in the polymer. The second or, in some instances, the third thermal scan was the actual thermogram used to determine the thermal expansion coefficient of the polymer. At the end of the first or second run, the sample was first cooled from 200°C to room temperature by itself and subsequently brought down to 0°C with the use of liquid nitrogen in the cooling jar surrounding the sample holder. Five or six specimens were measured for each polymer to determine its linear thermal expansion coefficients below and above the glass transition temperature.

Physical Testing

Dielectric Constant and Dissipation Factor

The dielectric constant and dissipation factor were measured by putting the polymeric film of each RME polymer between a sample holder, as shown schematically in Figure 2. After the formation of the capacitor with mercury as the electrode material, a 4192A LF Impedance Analyzer (Hewlett-Packard) was used to measure the dielectric constant and dissipation factor of the polymer at frequencies ranging from 10^2 to 10^7 Hz.

Solvent Swelling

Three specimens of known dimensions (about 12.7 × 50.8 × 0.3 mm) and weight (about 0.23–0.56 g) for each RME polymer were immersed in methyl ethyl ketone (Aldrich Chemical Co., Milwaukee, Wisconsin; density, 0.805 g/cm^3) at room temperature. The swollen specimen was weighed twice each

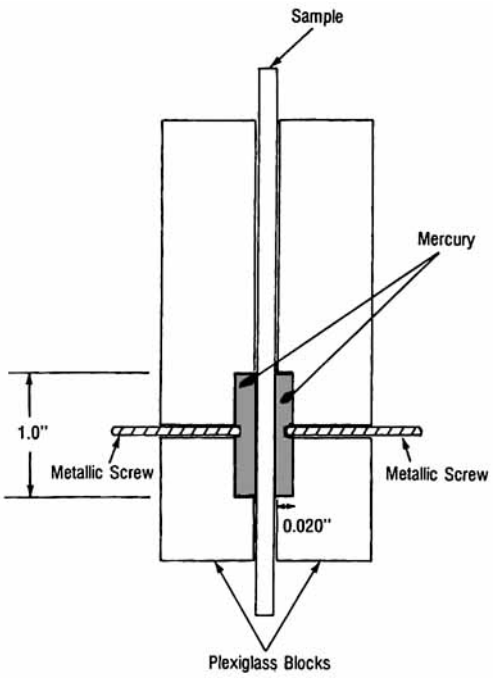

Fig. 2. Sample holder for dielectric constant measurements.

day until a fairly constant weight was attained. The specimen was finally vacuum dried in an oven at 80°C for 24 h and reweighed. This weight, W_o, is the actual weight of the dry polymer in the swollen state. If the original weight of the specimen is W, then the sol fraction is defined as

$$\text{Sol fraction} = (W - W_o) \times \frac{100\%}{W_o}$$

Stress-Strain Measurements

The tensile properties of the RME polymers were measured by using an Instron Tensile Tester. Test specimens were rectangular strips with width of 12.7 mm (0.5 in.). The crosshead speed used was 12.7 mm/s (0.5 in./s). Five specimens were tested for each polymer, and the final datum was the average of these measurements.

Friction

A method derived from ASTM D 1894[14] was used to determine the static and kinetic coefficients of friction of the RME polymers. A moving sled with a stationary plane, as shown in Figure 3, was employed.

The sled was a metal block with a length of 58.42 mm (2.30 in.), a width of 53.34 mm (2.10 in.), and a thickness of 6.35 mm (0.25 in.). A sponge rubber pad with the same length and width as the metal sled and a thickness of 3.81 mm (0.15 in.) was adhered to the bottom of the sled. The hardness,[15] measured by a Type A durometer (Pacific Transducer Corp., Los Angeles,

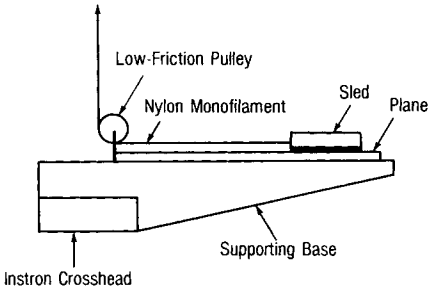

Fig. 3. Friction test (ASTM D 1894).

California), of the sponge rubber is A/23/1. The test specimen, in the form of a thin sheet, was cut to the same size as the sled and attached to the rubber pad by using double-faced tape. The total weight of the padded sled and specimen was about 153–155 g. The plane, a polished sheet of aluminum, provided a flat and smooth support for the specimen on the top of this plane.

An Instron machine (Floor Model: M82923) was used as the force-measuring device. The friction test was performed at room temperature. The sliding speed of the sled was 2.54 mm/s (6 in./min.).

The static coefficient of friction μ_s was calculated as

$$\mu_s = \frac{F_s}{N}$$

where F_s is the tangential force to initiate the motion of the sled and N is the initial normal force due to the total weight of the sled, the rubber pad, and the sample. On the other hand, the kinetic coefficient of friction μ_k was calculated as

$$\mu_k = \frac{F_k}{N}$$

where F_k is the tangential force to maintain a uniform sliding of the sled across the plane. Five specimens were measured for each sample, and the final datum was the average of these measurements.

Abrasion

A Taber Abraser, manufactured by Teledyne Taber (North Tonawanda, New York), was used to measure the abrasion resistance of the RME polymers. Figure 4 shows the operational diagram of the abraser. Essentially, the two oppositely rotating abrasive wheels wear a circular path in the power-rotated sample. Each wheel is loaded with 1.00 kg and presses against the specimen. This arrangement will reveal abrasion resistance at all angles relative to the surface textures of the material. A suction nozzle connected to a vacuum unit, not shown in this diagram, will continuously remove any abraded particles from the specimen surface during the run of the exper-

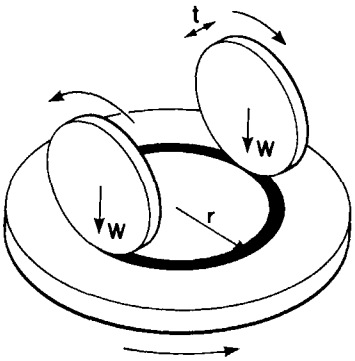

Fig. 4. Operation of Taber abraser; W = 1.00 kg, CS-17 wheels, t = wheel thickness = 1.3 cm, and r = mean radius of abraded circular path = 3.8 cm.

iment. The sample used in the run was a polymeric coating on top of an aluminum panel.

The turntable holding the specimen rotates at 72 rpm. The two abrasive wheels rotate at approximately 70 rpm, depending on the wheel diameter. The wheel diameter will diminish slightly after many runs. The CS-17 wheels used are a pair of resilient and coarse abrasive wheels. They are suitable for testing the abrasion resistance of most rigid polymers and plastic materials.

The specimen was abraded for 1000 cycles, and the associated weight loss was determined. Since different materials have different densities, it is better to consider the volume loss of the abraded polymers. In order to convert weight loss to volume loss, one needs to know the density of the different polymers being studied. The density of each polymer was determined by using the method of hydrostatic weighing. After each abrasion run, the CS-17 wheels must be refaced with a refacing stone to restore their abrading characteristics. Five abrasion specimens were measured for each polymer, and the final datum was the average of these measurements.

Scratch Hardness[16]

A set of calibrated wood pencils with a scale of hardness running from 6B to 6H, as shown in Figure 5A, was used. The sample used for each RME polymer in the test was a polymer-coated aluminum panel. A pencil was

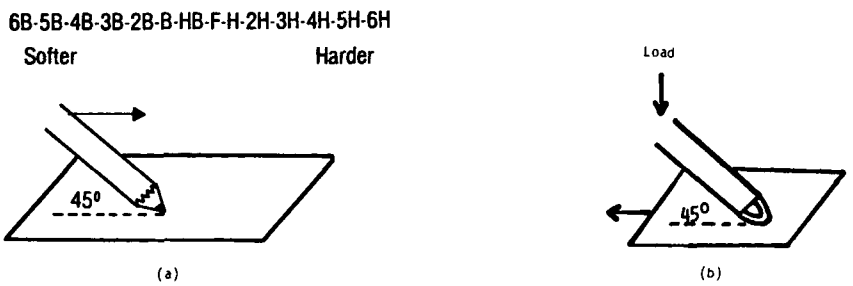

Fig. 5. (a) Pencil hardness (ASTM D 3363); (b) balanced-beam scrape-adhesion tester.

held firmly against the polymer surface at an angle of 45° (pointing away from the operator) and then pushed away from the operator in a ¼-in. stroke. The process was begun with the hardest pencil and carried on down the scale of hardness. Gouge hardness is the softest pencil that can cut through the sample film. Scratch hardness is the softest pencil that can scratch the surface of the sample.

Scrape Adhesion[17]

The scrape adhesion of the RME polymers to untreated aluminum panel was studied by using a modified balanced-beam scrape-adhesion tester with high loading force. The scraping loop was brought in contact with the specimen surface at an angle of 45°. The loop is a 1.59-mm (0.0625 in.) diameter drill rod, bent into a U shape, with an outside radius of 3.25 mm (0.128 in.). A load was applied, and the specimen was scraped a single stroke (Figure 5B). The scrape adhesion is defined as the minimum load applied, expressed in kilograms, to shear the polymeric coating from the substrate surface. Four specimens were measured for each polymer, and the final datum was the average of these measurements.

RESULTS AND DISCUSSION

EEW

The epoxy equivalent weight of the base epoxy resin, RMEO, which contained 7 wt % of Hycar liquid polymer, was found to be 970 $\pm$ 13 g/Eq based on the use of four specimens.

Thermal Analysis

DSC

Figure 6 shows the thermograms of the first and second runs of uncured RME10. The other uncured RME polymers exhibit similar heat flow versus temperature characteristics. Thermograms of the first and second runs and the third run of RMEO cured at 200°C for 15 min are shown in Figures 7 and 8, respectively. The rest of the RME polymers cured at the same schedule exhibits DSC traces similar to RMEO.

The DSC data are summarized in Table IV. Each heat of reaction of the curing exotherm is the apparent value with no correction accounting for the presence of filler. One would say that this exothermic energy decreases with increasing filler content. Also, the glass transition temperature of different fully cured polymers seems to be close to each other. This indicates the independence of T_g on the presence of filler. Data in the last two columns of Table IV imply that the cure condition of 200°C for 15 min is not sufficient for this polymeric system. Each polymer cured under this schedule shows lower T_g than its fully cured counterpart, which was obtained after the first run in the DSC cell. Actually, it was found that each polymer had the same T_g as observed in the second run even after a third or fourth thermal scan.

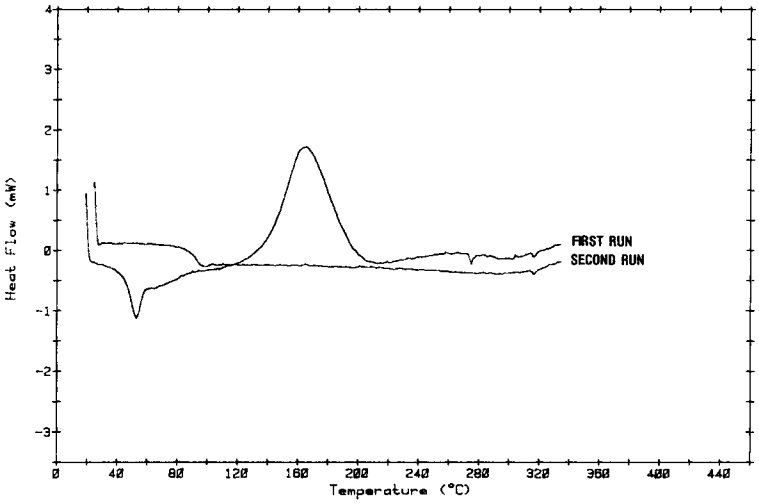

Fig. 6. DSC scans of uncured RME10.

According to Figure 8, it seems that there is no glass transition corresponding to the rubber phase for RMEO. This holds true for RME10, RME40, and RME60. At first glance, one may explain the disappearance of the rubber glass transition in the following manner. The initial curing of the polymers was set at a relatively high temperature for a short period of time (200°C for 15 min) to utilize the fast-cure nature of the curing agent. Therefore, cross-linking could proceed when both molten phases were mixed reasonably well together due to their relatively low molecular weights (as indicated probably by the EEW data). In the later stage of the 15 min, the viscosity increased very rapidly, and the system could not have enough driving force to phase separate due to subsequent restriction imposed by these rapidly developed cross-linking sites. However, from Figure 8 one can

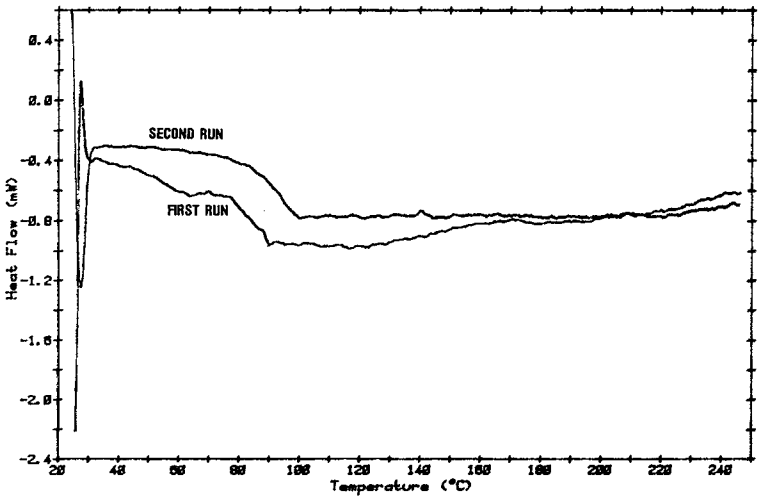

Fig. 7. DSC scans of RMEO cured at 200°C for 15 min.

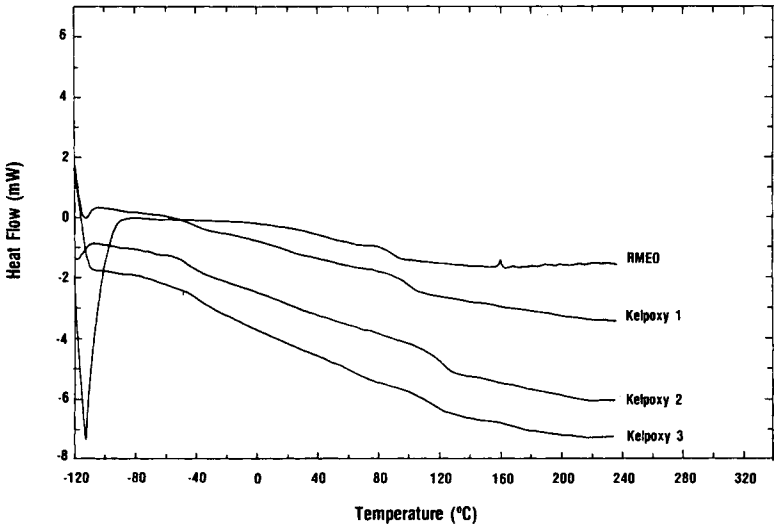

Fig. 8. The third DSC scan from −120 to 250°C.

detect two separate-glass transitions for the Kelpoxy polymers no matter whether accelerated dicyandiamide (under fast or slow cure) or DETA was used. Also, it seems that Kelpoxy polymer cross-linked under fast-cure conditions yields a lower T_g for the epoxy phase. The reason for the absence of T_g for the rubber phase in the RME polymers is not clear. The relatively low CTBN content (7 wt %) in these polymers may be insufficient to produce any detectable response in the DSC.

TGA

The filler content of the barium titanate-filled rubber-modified epoxies was verified by pyrolyzing the polymers under air atmosphere via TGA. The results are shown in Figure 9 and Table V. These air pyrolysates have weights close to the respective amounts of barium titanate mixed to the polymers. The decomposition temperature is the temperature at which the derivative of weight versus temperature curve reaches a maximum.

Figure 10 shows the thermograms of the different polymers pyrolyzed in a nitrogen atmosphere at a heating rate of 10°C/min. Each of these polymers

TABLE IV
DSC Results[a]

				Cured at 200°C for 15 min	
Polymer	T_g uncured (°C)	Heat of reaction (J/g)	T_g cured (°C)	T_g first run (°C)	T_g second run (°C)
RME0	43	86	84	48, 77	84
RME10	43	73	86	49, 77	85
RME40	45	50	86	49, 78	83
RME60	42	38	88	49, 76	87

[a] Heating rate, 5°C/min.

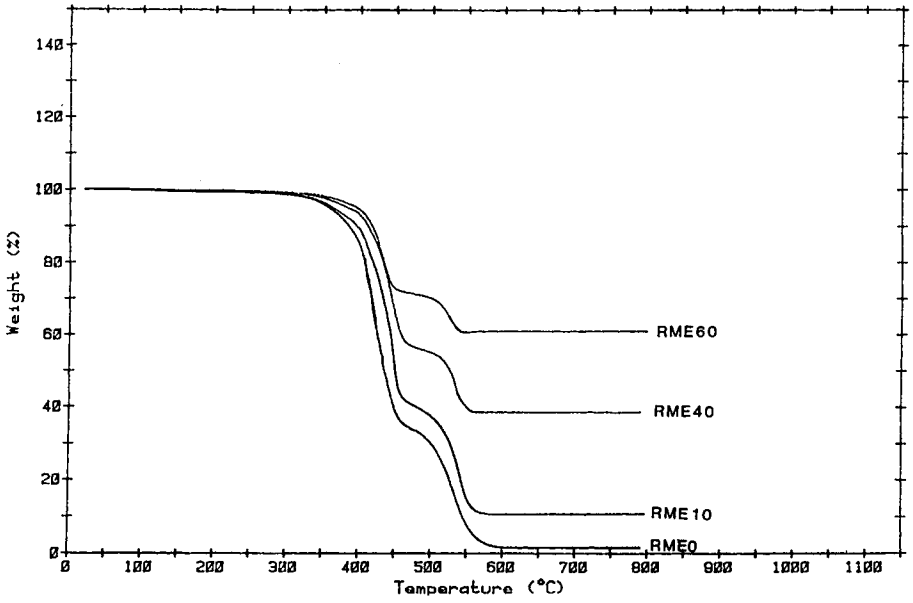

Fig. 9. Thermogravimetric pyrolysis in air for barium titanate-filled rubber-modified epoxy.

yielded a carbonaceous residue that arises from the heteroatoms, such as oxygen and nitrogen, in the polymer.

Figure 11 shows the thermograms of RMEO obtained at different heating rates. Usually a fast heating rate raises the temperatures for the onset of decomposition and expands the temperature range for the occurrence of weight loss. The activation energy of pyrolysis was determined according to the method devised by Reich.[18] With the assumption that the Arrhenius equation is valid in polymer pyrolysis, one may write

$$-\int_{W_o}^{W} \frac{dW}{W^n} \cong \frac{ART^2}{(RH)E} \exp\left(-\frac{E}{RT}\right),$$

$$\frac{W_o^{1-n}(1 - (W/W_o)^{1-n})}{1 - n} \cong \frac{ART^2}{(RH)E} \exp\left(-\frac{E}{RT}\right)$$

or

$$-\ln\frac{(RH)}{T^2} \cong \frac{E}{RT} + f(W, W_o, n)$$

TABLE V
TGA Results[a]

Polymer	N_2		Air	
	Decomposition temp. (°C)	Residue (wt %)	Decomposition temp. (°C)	Residue (wt %)
RME0	450	10	440, 540	2
RME10	450	21	450, 540	11
RME40	450	45	450, 540	39
RME60	430	65	440, 530	61

[a] Heating rate, 10°C/min.

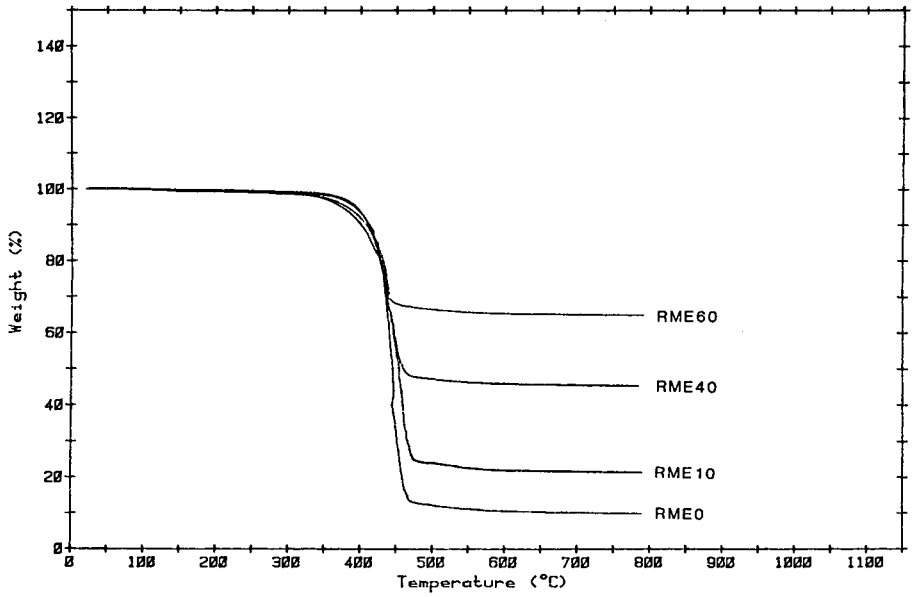

Fig. 10. Thermogravimetric pyrolysis in nitrogen for barium titanate-filled rubber-modified epoxy.

where W = weight of active material, W_o = initial weight of the active material, n = reaction order, A = frequency factor, (RH) = heating rate, R = universal gas constant, E = activation energy, and T = absolute temperature. The constancy of the last term on the *RHS* of the last equation relies on constant values of W_o, (W/W_o), and n for different values of (RH). As mentioned in the experimental section, W_o for each polymer was mon-

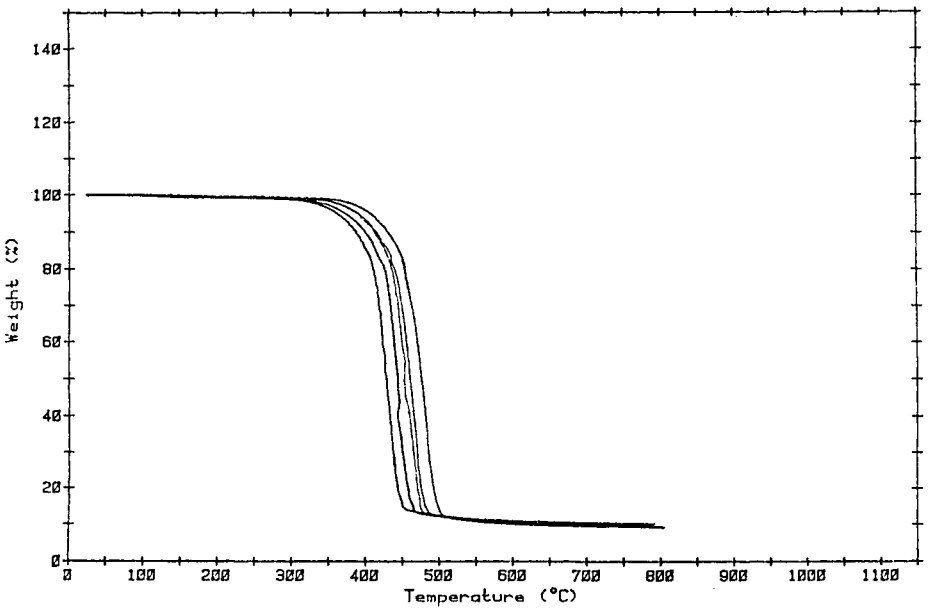

Fig. 11. Thermogravimetric curves for RMEO at various heating rates: 5, 10, 15, 20, and 30°C/min, from left to right. Sample weight, 15 ± 1 g; nitrogen atmosphere.

itored to be 15 ± 1 mg. By assuming the constancy of n at different rates and choosing various specific values of W, one can plot $-\ln[(RH)/T^2]$ versus $1/T$ to yield a series of nearly parallel lines whose slopes will be averaged to give the value of E. Figure 12 shows these plots for RMEO, and Table VI lists values of activation energy for the polymers. These are unmodified values with no correction made for the filler effect. From there, it seems that different polymers exhibit similar "apparent" activation energy of pyrolysis.

TMA

The linear thermal expansion coefficients below and above T_g, γ_g and γ_l, respectively, for each RME polymer are shown in Table VII. The error in each coefficient is the standard deviation of the several measurements obtained from each polymer. The temperatures within the brackets are the end points of the temperature range in which this coefficient is determined.

As one can see, the incorporation of 10 wt % (or higher) $BaTiO_3$ drops the value of γ_g by approximately 50%. It is surprising that this γ_g value does not decrease with further increase in filler content. However, above T_g, there is a continuous drop in linear thermal expansion coefficient with increasing filler level.

Dielectric Properties

In dielectric measurements an oscillating electrical field produces an oscillating electrical polarization, which usually lags the applied field by a phase angle δ defined by the dissipation factor

$$\tan \delta = \frac{\epsilon''}{\epsilon'}$$

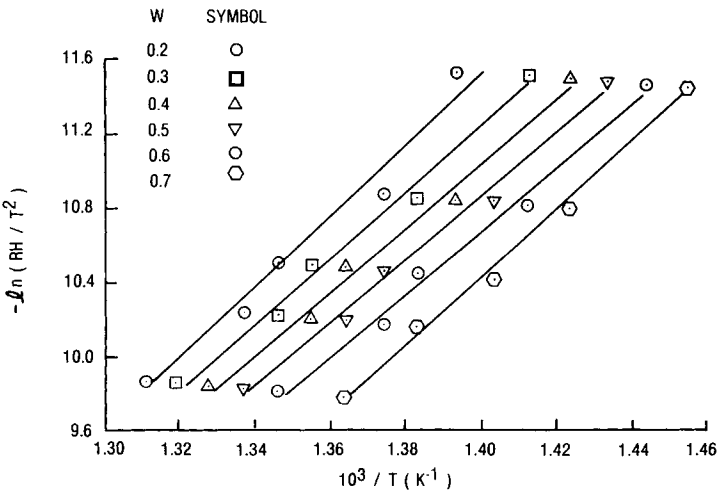

Fig. 12. Determination of activation energy for RMEO.

TABLE VI
Activation Energy of Pyrolysis

Polymer	E (kJ/mole)
RME0	151
RME10	176
RME40	160
RME60	156

where ϵ' and ϵ'' are the real and imaginary parts of the complex dielectric constant ϵ ($\epsilon = \epsilon' - i\epsilon''$). Figures 13–15 show the results of the dielectric measurements, where f denotes the frequency, and each error bar is the standard deviation of the several measurements made on each polymer.

It is immediately obvious from Figure 13 that ϵ' increases with the amount of barium titanate loaded at any given frequency. Also, as one can see, ϵ' drops with increasing frequency for each polymer. The rate of decrease of ϵ' with f seems to be in the order RME60 > RME40 > RME10 > RMEO. This is actually not true since the calculated value of the fractional change of ϵ' at a given frequency with respect to ϵ' at 100 Hz remains fairly constant when one polymer is compared to the others.

The value of tan δ seems to be quite independent of filler content in the rubber-modified epoxy systems, as shown in Figure 14. Actually, its value between 10^2 and 10^4 Hz is close to the reported value of 0.010–0.015 for barium titanate at 1 kHz. The values of ϵ'' at different frequencies deduced from data of ϵ' and tan δ are shown in Figure 15. It appears that ϵ'' increases with barium titanate loading at a given frequency, and all these curves show a common maximum at about 3.16×10^6 Hz, independent of the filler loading.

Solvent Swelling

The average molecular weight between cross-links, M_c, of each polymer was determined by using the Flory-Rehner equation[20] as shown below:

$$M_c = -\frac{V_1\rho_2(V_r^{1/3} - 0.5\ V_r)}{\ln(1 - V_r) + V_r + \chi V_r^2}$$

where V_1 = molar volume of solvent, ρ_2 = density of polymer, V_r = volume fraction of polymer in swollen gel, and χ = polymer-solvent interaction parameter. The volume fraction of polymer in the swollen network, V_r, was based only on the polymer matrix according to the equation

$$V_r = \frac{V_o - V_f}{V_s - V_f}$$

where V_o = volume of unswollen polymer, V_f = volume of filler in polymer, and V_s = volume of swollen polymer.

TABLE VII
Linear Thermal Expansion Coefficients

Material	$\gamma_g \times 10^6$ (°C^{-1})	$\gamma_l \times 10^6$ (°C^{-1})
RME0	49 ± 12 (19–67°C)	245 ± 29 (121–181°C)
RME10	25 ± 4 (20–61°C)	213 ± 16 (124–154°C)
RME40	25 ± 8 (15–61°C)	199 ± 13 (128–161°C)
RME60	27 ± 3 (14–60°C)	137 ± 7 (134–204°C)
$BaTiO_3$	7.0–10 (20–700°C)[19]	—

The χ value was determined from the semiempirical equation[21]

$$\chi = \chi_s + \frac{V_1(\delta_1 - \delta_2)^2}{RT}$$

where $\chi_s \approx 0.35$, δ_1 and δ_2 = solubility parameters of the solvent and polymer, respectively, and R = universal gas constant. In this case a χ value of 0.44 was obtained by assuming $\delta_1 = 9.3$ cal$^{1/2}$ cm$^{-3/2}$ for methyl ethyl ketone[22] and $\delta_2 = 10.9$ cal$^{1/2}$ cm$^{-3/2}$ for pure epoxy polymer.[22]

Values of V_r, $\mathbf{q}_m$, sol fraction, and M_c for the polymers are shown in Table VIII, where $\mathbf{q}_m$, the swelling ratio, is equal to V_r^{-1}. The sol fraction is based on the total weight of polymer and filler, assuming no loss in filler when the sample is swollen in the solvent. As one can see, the swelling ratio

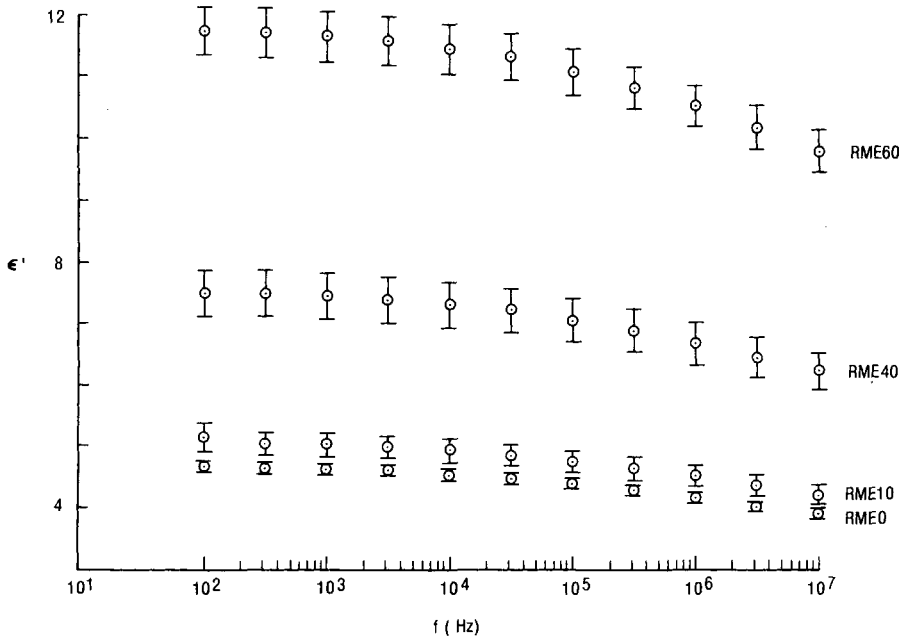

Fig. 13. Dependence of ϵ' on frequency for rubber-modified epoxy loaded with different amounts of barium titanate.

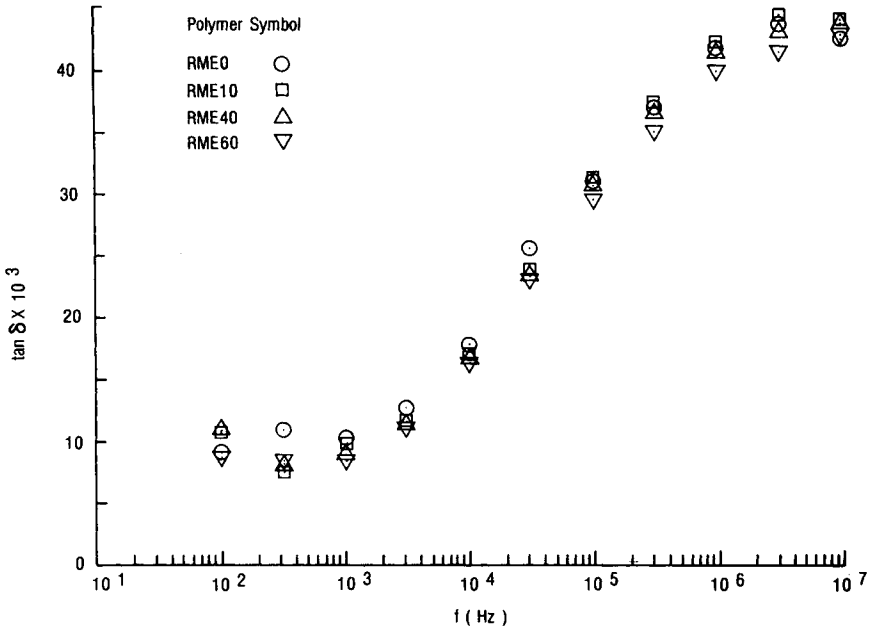

Fig. 14. Dependence of tan δ on frequency for rubber-modified epoxy loaded with different amounts of barium titanate.

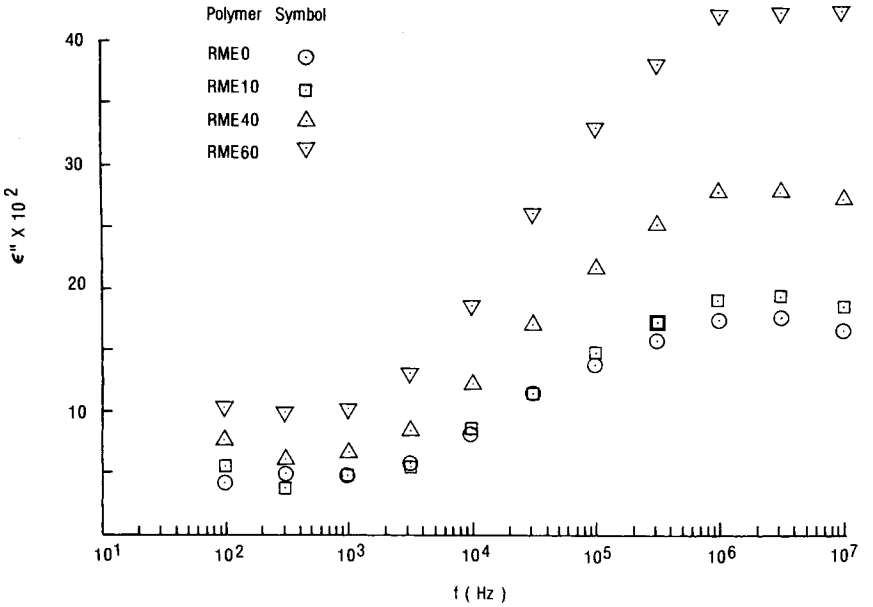

Fig. 15. Dependence of ϵ'' on frequency for rubber-modified epoxy loaded with different amounts of barium titanate.

TABLE VIII
Solvent Swelling of Polymers

Polymer	V_r	q_m	Sol fraction (%)	M_c (g/mole)
RME0	0.47	2.13	3.85	830
RME10	0.48	2.08	3.39	840
RME40	0.49	2.04	2.56	1000
RME60	0.52	1.92	2.14	1200

decreases with the amount of barium titanate loaded in the polymer. However, a number of investigators[23-27] have studied the swelling measurements of filled elastomers and found that the swelling ratio either decreases or does not vary with filler content.

Table VIII indicates that both the degree of cross-linking and sol fraction decrease with barium titanate content in the polymeric network. The first observation may be explained by assuming that filler hinders the efficiency of the curing agent. Why sol fraction decreases with filler content is not clear. Also, one would say that cross-linking density of the epoxy polymers does not affect T_g, as indicated by DSC results.

Stress-Strain Properties

The stress-strain curves and some important tensile properties of the RME polymers are shown in Figure 16 and Table IX, respectively. As one can see, the higher the filler content, the higher are the modulus and tensile strength, although the latter quantity only rises slightly. On the other hand, the elongation at break of the polymer decreases with filler addition. Only

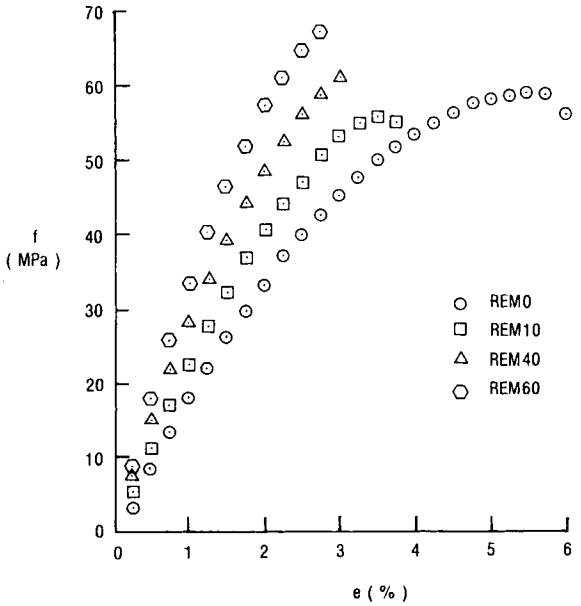

Fig. 16. Stress-strain relation at room temperature and at initial strain rate of 4.16 × 10^{-3} s^{-1}.

TABLE IX
Tensile Properties

Polymer	Modulus of elasticity (GPa)	Tensile strength (MPa)	Yield stress (MPa)	Elongation at break (%)
RME0	1.78	56	59	6.00
RME10	2.25	55	56	3.75
RME40	2.85	61	—	3.00
RME60	3.35	67	—	2.75

RMEO and RME10 show the existence of a yield point shortly before rupture.

The strength enhancement to elastomers contributed by filler has been the subject of intensive study for a great number of years.[28-35] It has been concluded by Gent[28,29] that hysteresis,[30-33] stiffness,[34] and tear deviation[35] are the three main mechanisms for the reinforcing ability of fine-particle fillers in rubbers. It is believed that enhanced strength of barium titanate-filled epoxy could also be explained by the same set of mechanisms. However, the filled epoxy is not greatly reinforced, probably due to the small contribution from hysteresis because of the nonbonding nature of polymeric matrix and barium titanate particles. A final word about the rupture properties of the epoxy polymers is that the more densely cross-linked polymer, as indicated by swelling data, may not necessarily have higher tensile strength and lower value of elongation at break.

Friction and Abrasion

The friction and abrasion data are summarized in Table X, where ρ is the density, ΔW is weight loss of the specimen per 1000 abrasion cycles, ΔV is the associated volume loss, and the abradability[36] is defined as the volume abraded away per unit normal load and unit sliding distance divided by the coefficient of friction. The error in ΔW is the standard deviation of the several measurements obtained from each polymer.

The density of barium titanate-filled rubber-modified epoxy increases with filler content. As one can see, the first three polymers seem to have a similar coefficient of friction. The friction of RME60 is even lower than that of the rubber-modified epoxies with lower filler contents, namely,

TABLE X
Friction and Abrasion of Polymers

Polymer	ρ(g/cm^3)	μ_s	μ_k	$\Delta W \times 10^3$ (g)	$\Delta V \times 10^3$ (cm^3)	(Abradability) $\times 10^{12}$ (Pa^{-1})
RME0	1.1568 ± 0.0068	0.32	0.23	10.7 ± 1.7	9.2 ± 1.5	8.56
RME10	1.2540 ± 0.0180	0.34	0.22	11.3 ± 0.5	9.0 ± 0.4	8.77
RME40	1.6748 ± 0.0184	0.32	0.24	22.1 ± 2.2	13.2 ± 1.3	11.74
RME60	2.2553 ± 0.0060	0.20	0.13	32.6 ± 9.0	14.4 ± 4.0	23.65
Mylar EL	1.3760 ± 0.0135	0.43	0.26	25.7 ± 3.7	18.6 ± 2.7	15.20
Kapton H	1.4280 ± 0.0083	0.45	0.27	11.7 ± 3.2	8.2 ± 0.6	6.45

RMEO, RME10, and RME40. The difference in friction may be attributed to the different fabrication methods: RMEO, RME10, and RME40 were prepared via fluidized-bed coating; RME60 was prepared via compression molding. Each polymer exhibits a static coefficient of friction greater than its kinetic coefficient of friction, resulting in slipstick motion. This is actually what was observed during the friction tests.

The standard deviation of ΔV, $S(\Delta V)$, in Table X was calculated according to the basic formula for error propagation:[37]

$$S(\Delta V) = \Delta V\left[\left(\frac{S\ (\Delta W)}{\Delta W}\right)^2 + \left(\frac{S(\rho)}{\rho}\right)^2\right]^{1/2}$$

where $S(\Delta W)$ and $S(\rho)$ are the standard deviations of ΔW and ρ, respectively. In the calculations of the abradability, the coefficient of friction between the polymer and the abrading wheel was assumed to be μ_k, the kinetic coefficient of friction of the polymer with itself.

As one can see, it appears that higher loading of barium titanate is deleterious to the abrasion resistance of the polymers. As mentioned, filled polymers usually have higher strength and tearing resistance than their corresponding unfilled materials due to the occurrence of stress softening and deviation of tear path in the reinforced systems. The process of abrasion may be viewed as the detachment via small particle tearing under the mechanical action of friction. Then, why are the filled polymers less abrasion resistant? Gent[29] put forward the following explanation. The small particle tearing that occurred in abrasion probably does not have any lateral deviation due to the restriction of the abrading scale on that part of the sample where tearing occurs. It has been found that the abrasion resistance of reinforced elastomers is generally smaller than that of their unfilled counterparts.

Data for two commercial polymeric films, Mylar EL (DuPont's biaxial-oriented polyethylene terephthalate) with thickness of about 190 μm (7.5 mils), and DuPont's type H Kapton polyimide with thickness of about 76 μm (3 mils), are also included in Table X for comparison with the epoxy polymers. One would notice the high abrasion resistance of the polyimide film.

Scratch Hardness and Scrape Adhesion

Table XI summarizes the results of the scratch hardness and scrape adhesion measurements. All the polymers exhibit a gouge hardness equal to or greater than 6H. The scratch hardness increases with barium titanate content for the epoxy polymers. As one can see from the scratch hardness and abrasion data, poor scratch resistance does not necessarily imply poor abrasion or wear in terms of abradability from Taber volume loss. Rubber-modified epoxy with a higher loading of barium titanate has higher scratch hardness but poorer abrasion resistance. On the other hand, polyimide has low scratch hardness, but its abrasion resistance is surprisingly high. A

TABLE XI
Scratch Hardness and Scrape Adhesion

Polymer	Coating thickness (μm)	Gouge hardness	Scratch hardness	Scrape adhesion (kg)
RME0	117	>6H	H	26
RME10	74	>6H	3H	23
RME40	81	>6H	3H	24
RME60	99	>6H	4H	43
Mylar EL	190	>6H	H	—
Kapton H	76	>6H	3H	—

classic example is polyethylene. Polyethylene is easily scratched due to its low hardness, but it has very low abrasion loss by some tests.[38]

The scrape adhesion could be considered, more or less, as a combined process of indentation and tearing. The loaded loop has to indent into the polymeric coating before any tearing of the polymer from the substrate occurs. The slightly higher scrape adhesion of RMEO compared with those of RME10 and RME40 can probably be explained by the fact that unfilled polymer usually has a higher adhesion to metal substrate than the filled compound. However, increasing filler content increases the hardness of the polymeric compound, as exemplified by the scratch hardness in this case. This makes the indentation process more dominant than the tearing process, resulting in high scrape adhesion of RME60. Peel strength measurements of the polymeric coating on the aluminum substrate was difficult for these polymers due to the extremely strong adhesion of the polymers to the above substrate and the brittle nature of the polymers.

CONCLUSIONS

The presence of barium titanate in rubber-modified epoxy does not affect the glass transition temperature and the activation energy of pyrolysis of the polymer.

The filled rubber-modified epoxies with different loadings of barium titanate seem to have a similar thermal expansion coefficient below the glass transition temperature T_g of the polymers. However, thermal expansion of the polymers decreases with filler content above T_g.

The dielectric constant increases markedly, but the dissipation factor remains fairly constant with increasing barium titanate loading in the rubber-modified epoxy system.

Both the degree of cross-linking and sol fraction decrease with barium titanate content in the polymeric network, as indicated by equilibrium swelling in MEK.

The presence of barium titanate increases the modulus of elasticity and tensile strength but decreases the elongation of break of the thermosetting polymer.

It seems that higher loading of barium titanate is deleterious to the abrasion resistance of the rubber-modified epoxy. A lower coefficient of friction and/or higher scratch hardness do not necessarily imply good abrasion resistance in terms of abradability from Taber volume loss.

The barium titanate-filled rubber-modified epoxy was first developed by W. A. Romanchick (now at Betz Laboratories, Inc.) and J. F. Geibel (now at Phillips Petroleum). The author wishes to thank L. G. Frank for the sample preparation, E. L. Bogatin for the dielectric constant measurements, and H. M. Zupko of Bell Laboratories, AT&T Technologies, for allowing him to perform some of the mechanical tests in his laboratory. He also likes to acknowledge the kind permission of AT&T for publishing this work.

References

1. F. J. McGarry and J. N. Sultan, Research Report R67-66, Massachusetts Institute of Technology, 1967.
2. F. J. McGarry and A. M. Willner, Research Report R68-8, Massachusetts Institute of Technology, 1968.
3. F. J. McGarry, A. M. Willner, and J. N. Sultan, Research Report R69-59, Massachusetts Institute of Technology, 1969.
4. E. H. Rowe, A. R. Siebert, and R. S. Drake, *Mod. Plastics,* **47**, 110 (1970).
5. J. N. Sultan and F. J. McGarry, *Polym. Eng. Sci.,* **13**, 29 (1973).
6. A. C. Meeks, *Polymer,* **15**, 675 (1974).
7. S. C. Kunz, J. A. Sayre, and R. A. Assink, *Polymer,* **23**, 1897 (1982).
8. W. A. Romanchick, J. E. Sohn, and J. F. Geibel, *ACS Symposium Series 221,* American Chemical Society, Washington, D.C., 1983, pp. 85–118.
9. W. D. Kingery, H. K. Bowen, and D. R. Uhlman, *Introduction to Ceramics,* 2nd ed., John Wiley & Sons, New York, 1976, pp. 967–972.
10. A. R. von Hippel, *Dielectrics and Waves,* John Wiley & Sons, New York, 1954, pp. 202–213.
11. *Ticon Barium Titanate Product Information,* Tam Ceramics, Inc., Niagara Falls, New York.
12. *TD-79104,* Spencer Kellog Division, Textron Inc., Buffalo, New York, December 18, 1984.
13. R. R. Jay, *Anal. Chem.,* **36**, 667 (1974).
14. ASTM Spec. D 1894-78, American Society for Testing and Materials, Philadelphia, 1978.
15. ASTM Spec. D 2240-75, American Society for Testing and Materials, Philadelphia, 1975.
16. ASTM Spec. D 3363-74, American Society for Testing and Materials, Philadelphia, 1974.
17. ASTM Spec. D 2197-68, American Society for Testing and Materials, Philadelphia, 1968.
18. L. Reich, *Polym. Lett.,* **2**, 621 (1964).
19. *Dielectric Materials and Applications,* A. R. von Hippel, Ed., John Wiley & Sons, New York, 1954, p. 181.
20. P. J. Flory, *Principles of Polymer Chemistry,* Cornell University Press, Ithaca, New York, 1953, p. 579.
21. J. H. Hildebrand and R. L. Scott, *The Solubility of Nonelectrolytes,* 3rd ed., Dover, New York, 1950, pp. 361–367.
22. *Polymer Handbook,* 2nd ed., J. Brandup and E. H. Immergut, Eds., John Wiley & Sons, New York, 1975, Chapter IV, pp. 337–359.
23. K. H. Bills, Jr., and F. S. Salcedo, *J. Appl. Phys.,* **32**, 2364 (1961).
24. G. Kraus, *J. Appl. Polym. Sci.,* **7**, 861 (1963).
25. R. F. Fedors and R. F. Landel, *J. P. L. Space Programs Summ.,* 37–40, IV 80 (1966).
26. R. Dick, G. Mavel, and R. Mankowski-Favelier, *Colloq. Int. Centre Nat. Rech. Sci.,* **231**, 165 (1975).
27. Y. Eckstein and P. Dreyfuss, *J. Polym. Sci., Polym. Phys. Ed.,* **20**, 49 (1982).
28. A. N. Gent, *Polymer Science and Materials,* A. V. Tobolsky and H. F. Mark, Eds., Wiley Interscience, New York, 1971, pp. 275–305.
29. A. N. Gent, *Fracture,* Vol. VII, H. Liebowitz, Ed., Academic Press, New York, 1972, pp. 315–350.

30. R. Houwink, *Rubb. Chem. Technol.*, **29**, 888 (1956).
31. F. Bueche, *J. Appl. Polym. Sci.*, **4**, 107 (1960).
32. J. A. C. Harwood, L. Mullins, and A. R. Payne, *Polym. Lett.*, **B3**, 119 (1965).
33. J. A. C. Harwood, L. Mullins, and A. R. Payne, *J. Appl. Polym. Sci.*, **9**, 3011 (1965).
34. J. C. Halpin and F. Bueche, *J. Appl. Phys.*, **35**, 3142 (1964).
35. E. H. Andrews, *J. Appl. Phys.*, **32**, 542 (1961).
36. K. A. Grosch and A. Schallamach, *Wear*, **4**, 356 (1961).
37. P. R. Bevington, *Data Reduction and Error Analysis for the Physical Sciences*, McGraw-Hill, New York, 1969, p. 56.
38. L. E. Nielsen, *Mechanical Properties of Polymers and Composites*, Vol. 2, Marcel Dekker, New York, 1974, p. 362.